PFC/JA-92-19

Effect of Anomalous Alpha Diffusion on Fusion Power Coupling into Tokamak Plasma

D. J. Sigmar, R. Gormley, and G. Kamelander*

June 1992

Plasma Fusion Center

Massachusetts Institute of Technology

Cambridge, MA 02139 USA

---

* Zentralforschungsanstalt Seibersdorf and Technical University of Vienna, Austria

EFFECT OF ANOMALOUS ALPHA DIFFUSION ON FUSION POWER COUPLING INTO TOKAMAK PLASMA

D. J. Sigmar, R. Gormley, and G. Kamelander*

Massachusetts Institute of Technology

Plasma Fusion Center

Cambridge, Massachusetts 02139 USA

Abstract

The α power coupling efficiency $\eta_\alpha \equiv P_\alpha$ (coupled)$/P_\alpha$ (birth) is reduced when the energetic alphas are subject to anomalous radial diffusion, D_α^{an} caused by α instabilities. $\eta_\alpha < 1$ can have a strong effect on the fusion yield Q [$\equiv P_{fusion}$ (out)$/P_{aux}$ (in)]. First, a simple analytic form of η_α is found to be $\eta_\alpha = 1 - \frac{\nu_L \tau_{SD}}{2 + \nu_L \tau_{SD}}$ where $\nu_L \simeq \frac{4 D_\alpha}{a^2}$ is the spatial loss frequency and τ_{SD} is the slowing down time. η_α decreases with T_e and increases with n_e. Second, a reduced time dependent α kinetic equation containing the term $\nabla \cdot D_\alpha \nabla n_\alpha$ where D_α is a nonlinear function of $\partial n_\alpha / \partial r$ is derived and solved using a multi-energy group method. A turbulent theory by F. Gang (Phys. Fluids B4, 1992, accepted for publication) is used to parametrize D_α from first principles. η_α is reduced to 0.9 when $D_\alpha^{an} \simeq 1$ m^2/s and further consequences for the accessible operating regimes are discussed, including the effect of D_α^{an} on Q.

* Zentralforschungsanstalt Seibersdorf and Technical University of Vienna, Austria

I. Introduction

It is usually assumed that (with the exception of a very small fraction of prompt orbit losses and a small fraction of toroidal field ripple losses) the fusion born α particles are nearly perfectly confined during their slowing down by electron drag to the critical energy, thus delivering almost all of the α power at birth $P_\alpha^{(0)} = S_f E_{\alpha o} = n_D n_T \langle \sigma_f v \rangle E_{\alpha o}$ to the background plasma. While the notion of an anomalous radial diffusion coefficient D_α^{an} of the fast alphas was introduced some time ago [1-4], the impact of such losses on burning plasma performance has only been addressed recently [5]. In Ref. [5] it is shown that the α power coupling ratio $\eta_\alpha \equiv P_\alpha^{eff}/P_\alpha^{(0)}$ (where P_α^{eff} is the power of the confined alphas actually coupling into the bulk plasma) has a sensitive influence on the achievable thermonuclear Q.

In the present paper, we will investigate the dependence of η_α on D_α^{an} first analytically in Section II and second numerically in Section III, adopting theoretical and experimental values for D_α^{an} from known instabilities. In Section IV we will discuss the ensuing values for η_α and its effect on thermonuclear Q and plasma operations contour. A summary section concludes the work.

II. Relation between D_α^{an} and η_α

II.1 Analytic model

Let

$$P_\alpha^{eff} \equiv \eta_\alpha P_\alpha^{(0)} \equiv - \int d^3v \frac{m_\alpha v^2}{2} C_\alpha(f_\alpha) \tag{1}$$

where C_α is the (dominant) collisional electron drag operator. The α distribution function results from the model kinetic equation (replaced by a rigorous equation below)

$$\nu_L f_\alpha = C_\alpha(f_\alpha) + S_f \frac{\delta(v - v_{\alpha o})}{4\pi v^2} \tag{2}$$

2

Here, $\nu_L = \frac{4D_\alpha^{an}}{a^2}$ describes the energy dependent anomalous α diffusion loss and $C_\alpha(f_\alpha) = \frac{1}{\tau_{SD}} \frac{\partial}{\partial v} \cdot \left(1 + \frac{v_c^3}{v^3}\right) \mathbf{v} f_\alpha$. Using (2) in (1) yields

$$\eta_\alpha = 1 - \frac{\overline{\nu_L n_\alpha E_\alpha}}{E_{\alpha o} S_f}.$$

(3a)

Here, $S_f = n_D n_T \langle \sigma_f v \rangle$ and the overbar denotes the energy average

$$\overline{\nu_L n_\alpha E_\alpha} = \int d^3 v \frac{m_\alpha v^2}{2} f_\alpha \nu_L(E).$$

(3b)

Note that f_α is the solution of Eq. (2) including the effects of $\nu_L \neq 0$:

$$f_\alpha = \frac{S_f \tau_{SD} H(v_{\alpha o} - v)}{4\pi (v^3 + v_c^3)^\mu} \left(v_{\alpha o}^3 + v_c^3\right)^{\mu - 1}$$

(4)

with $\mu \equiv 1 - \nu_L \tau_{SD}/3$ and H the Heavyside step function. Inserting (4) in Eqs. (3) yields

$$\eta_\alpha = 1 - \frac{\nu_L \tau_{SD}}{2 + \nu_L \tau_{SD}}.$$

(4a)

In cases where $\nu_L \tau_{SD} \ll 1$, this becomes

$$\eta_\alpha \simeq 1 - 0.62 \times 10^{20} \frac{T_e^{3/2}}{n_e} \nu_L.$$

(4b)

Here we used $\tau_{SD} = 1.24 \times 10^{18} T_e^{3/2}/n_e$ where n_e is in m^{-3} and T_e in KeV. Thus, since $\nu_L \tau_{SD}$ is an increasing function of T_e, the coupling efficiency η_α will be strongly reduced as T_e increases; on the other hand high n_e helps (see Fig. 8b showing curves of constant η_α in $n - T$ space, for an ITER-like machine). For the simple case where $D_\alpha = 1.0$ m^2/sec with a thermal background of $T_e = 10$ keV and $n_e = 1.0 \times 10^{20}/$m^3 $\eta_\alpha = 0.91$.

Equations (3a,b) give the basic relation between the anomalous diffusion loss and η_α. In a subsequent section we will solve Eqs. (2,3) numerically with a realistic diffusion term replacing $\nu_L f_\alpha$.

II.2 Kinetic Equation including Radial Diffusion and Reduction to Two Dimensions

In order to completely describe fast α thermalization it is necessary to include the competition between collisional slowing down and radial diffusion. This was done early on [6] by including the loss term $\nu_L f_\alpha$ in the kinetic equation. Düchs and Pfirsch [7] presented a heuristic form of the pitch angle averaged and flux averaged drift kinetic equation for f_α, containing the energy dependent radial diffusion term $\frac{1}{r}\frac{\partial}{\partial r}(F_\alpha \frac{\Gamma_\alpha}{n_\alpha})$, where $F_\alpha = F_\alpha(r, E)$; and $\Gamma_\alpha = \langle n_\alpha V_{\alpha r}\rangle$ is the self-consistent diffusion flux. Their kinetic equation is

$$\frac{\partial F_\alpha}{\partial t} + \nabla \cdot (F_\alpha \mathbf{V}_\alpha) + \nabla \cdot \left(F_\alpha \frac{\mathbf{q}_\alpha}{n_\alpha T_\alpha} \right)$$

$$= -\frac{\partial}{\partial E}(L F_\alpha) + \frac{\partial^2}{\partial E^2}(D F_\alpha) + S_f \delta(E - E_{\alpha o}). \tag{5}$$

Here, the heat flux term $\nabla \cdot (F_\alpha \mathbf{q}_\alpha)$ is included ad hoc, which will be discussed below. The Düchs/Pfirsch model has been further developed (including the replacement of $f_\alpha = \sum_\nu F^\nu_{Maxw}$ by a slowing down distribution) and used by Kamelander [8]. Attenberger and Houlberg [9] developed an alternative approach to solve the partial differential equation (5) using a multi-energy group system of coupled equations for $n^j_\alpha(r, E_j, t)$ in which collisional slowing down from energy group $j - 1$ to group j is balanced against a radial diffusion loss $\nabla \cdot \Gamma_j$, where $\Gamma_j = -D_j \cdot \nabla n_j$ and n_j is the differential number density in $[E, E + dE]$ corresponding to $F_\alpha(r E)$. Anderson et al [10] used a model α kinetic equation containing a radial diffusion term similar to Düchs/Pfirsch and applied it to the triton burnup problem in order to determine what level of anomalous fusion product diffusion is necessary to explain the missing tritons.

Clearly, it is desirable to find a rigorous but reduced kinetic equation. Starting from first principles, A. Ware [11] showed that averaging the ion drift kinetic equation

$$v_\| \nabla_\| f_i + \mathbf{v}_D \cdot \nabla f_i = C(f_i) \tag{6}$$

4

over the pitch angle variable $\mu B_0/E$ and over a flux surface which annihilates the first term in (6) yields

$$\frac{1}{r}\frac{\partial}{\partial r}r\Gamma_E = \int_0^{2\pi}\frac{d\theta}{2\pi}\int_0^{E/B_{min}}\frac{Bd\mu}{|v_\parallel|}C(f_i) \qquad (7a)$$

where

$$\Gamma_E = \int_0^{2\pi}\frac{d\theta h}{2\pi}\int_0^{E/B_{min}}\frac{Bd\mu}{|v_\parallel|}\,v_{dr}f_i. \qquad (7b)$$

Then, working out the averaged collision operator on the right hand side of (3a) leaves only energy derivatives of the form

$$\frac{\partial}{\partial E}LF - \frac{\partial^2}{\partial E^2}DF$$

as given in Eq. (5). Here, $F = F(r, E, t)$ is an averaged distribution function; and Γ_E is the particle flux in the energy interval $E, E + dE$, related to the particle cross field flux through

$$\Gamma = \int_0^\infty 4\pi\Gamma_E dE.$$

First, we mention two exact cases for Γ_E.

(i) For the neoclassical banana regime solution of the drift kinetic equation, Ref. [11] gives the result

$$\Gamma_E = -\int\int\frac{mv_\parallel h}{eB_\theta}C(f_i)\frac{Bd\mu}{|v_\parallel|}\frac{d\theta}{2\pi} \qquad (8a)$$

where $h = B_0/B = 1 + \epsilon\cos\theta$, and the rest of the notation is standard. Specifically, after inserting the standard banana regime solution for f_i, Γ_E takes on the form

$$\Gamma_E = -.49\left(\frac{r}{R}\right)^{1/2}\frac{m^2\nu_{pa}v^3}{e^2B_{\theta_o}^2}\frac{\partial f_0}{\partial r} \qquad (8b)$$

where ν_{pa} is the pitch angle scattering frequency. Integrating (8b) over energy $E = mv^2/2$ (cf. (7)) leads to the standard result for the flux averaged banana regime particle flux.

(ii) The result Eq. (8b) was based on a Maxwellian f_0. The analogous calculation of Γ_α for energetic alphas using the slowing down distribution $f_0 = f_{SD}$ and the rigorous pitch angle scatttering response f_1 was worked out by Hsu et al [12].

5

To understand the nature of the Düchs/Pfirsch model equation, we compare the heuristic kinetic equation of [7] with the exact equation (6) of Ware [11], and find

$$\langle \nabla \cdot F_\alpha \frac{\Gamma_\alpha}{n_\alpha} \rangle_{DP} = \langle \nabla \cdot \frac{d\Gamma}{dE} \rangle_{Ware} \qquad (9a)$$

or

$$\frac{1}{r} \frac{d}{dr} r \langle F_\alpha \frac{\Gamma_\alpha}{n_\alpha} \rangle = \frac{1}{r} \frac{d}{dr} r \overline{\langle \overline{f_\alpha v_{dr\alpha}} \rangle} \qquad (9b)$$

where $\langle \ \rangle$ denotes the flux average and the double overbar denotes the average over all pitch angles, cf. Eq. (7b). Equation (9b) reveals the nature of the approximation used in Ref. [7], which is to break up the pitch angle average

$$\overline{\langle \overline{f_\alpha v_{dr\alpha}} \rangle} \simeq \langle \overline{\overline{f}}_\alpha \rangle \langle \overline{\overline{v}}_{dr\alpha} \rangle \simeq \langle \overline{\overline{f}}_\alpha \rangle \frac{\Gamma_\alpha}{\langle n_\alpha \rangle} \qquad (10)$$

where Γ_α is the flux averaged radial flux. This approximate break up of $\overline{\langle \overline{f_\alpha v_{dr\alpha}} \rangle}$ will fail in the trapped/circulating particle transition layer which has been shown in Ref. [13] to contribute substantially to α particle neoclassical diffusion. (Similar to A. Ware, Goloborodko and Yavorskii [13] also apply bounce averaging to the drift kinetic equation. If one averages their Eq. (33) over pitch angle $\lambda = \mu B_0/E$, the result is closely related to Ware's.) Nevertheless, the breakup facilitates the reduction of the 4-D exact α kinetic equation to 2-D namely, $F_\alpha = F_\alpha(r, E)$, which is necessary to make the problem numerically tractable. This was the motivation of Düchs' and Pfirsch's and Anderson et al's very useful approach. But the heat flux term in [7] cannot be justified from the rigorous derivation given by Ware. If included, it should be considered as part of the particle flux model term, allowing more energy dependence to enter. In Refs. [8], this heat flux term allows for an energy dependent thermal conductivity $\chi = \chi(E)$ and is carefully constructed such that the energy moment over the model kinetic equation obeys an energy conservation law.

Finally, the multi-energy group method of Ref. [9] can be justified in view of the rigorous kinetic Eq. (7). For α particles, this becomes

$$\frac{\partial F_\alpha}{\partial t} + \frac{1}{r} \frac{\partial}{\partial r} r \Gamma_{E\alpha} = \langle \overline{\overline{S}}_f \rangle + \langle \overline{\overline{C}}_\alpha \rangle. \qquad (11)$$

6

Attenberger and Houlberg solve Eq. (11) via the discretized system

$$\frac{\partial n_j}{\partial t} - \frac{1}{r}\frac{\partial}{\partial r}rD_j\frac{\partial n_j}{\partial r} = S_{fj} + \frac{n_{j-1}}{\tau_{s,j-1}} - \frac{n_j}{\tau_{s,j}}. \tag{12}$$

Here, $n_j = n_j(r, E_j, t) = \int_{j+1}^{j} F_\alpha dE$ is the differential α density in the j-th energy group (with $j = 1$ for $E_1 = E_{\alpha 0} = 3.5$ MeV) and the diffusion term in Eq. (10) corresponds to Eq. (7b). The fusion source term S_f enters only in the highest energy group. Thus, we use a Fick's law of the form

$$\Gamma_{E\alpha} = -D_\alpha(E)\frac{\partial}{\partial r}\int_{j+1}^{j} F_\alpha dE \tag{13}$$

where $D_\alpha(E)$ comes from various α transport models. Also, $\tau_{s,j}$ is the slowing down time $\int_{j}^{j+1} dE/(dE/dt)$ of alphas in energy group j, and the energy diffusion term in the collision operator has been neglected (valid for $E_\alpha \geq E_{crit}$). The same breakup of the pitch angle average as discussed in Eq. (10) occurs in Eq. (11), and the effect of the trapped/passing orbit layer is also neglected in the present work.

II.3 Solution of the Reduced Kinetic Equation

Taking the energy moment of the reduced slowing down kinetic equation

$$\frac{\partial F_\alpha}{\partial t} = \frac{1}{\tau_{SD}v^2}\frac{\partial}{\partial v}\left[\left(v^3 + v_c^3\right)F_\alpha\right] + \frac{1}{r}\frac{\partial}{\partial r}\left(rD_\alpha\frac{\partial F_\alpha}{\partial r}\right) + \frac{S_f}{4\pi v_{\alpha 0}^2}\delta(v - v_{\alpha 0}) \tag{14}$$

gives

$$\overline{\nu_L n_\alpha E_\alpha} \equiv -\int d^3v\frac{m_\alpha v^2}{2}\frac{1}{r}\frac{\partial}{\partial r}\left(rD_\alpha\frac{\partial F_\alpha}{\partial r}\right). \tag{15}$$

Since we will see that D_α is a function of F_α, Eq. (14) is a nonlinear partial differential equation in three variables, r, v and t. Since all α particles are born at a single energy $= 3.52$ MeV and since over time they simply slow down to lower energies, a multiple energy group method was chosen for the solution. Attenberger and Houlberg [9] have shown that for the resulting set of discretized equations one needs only as few as 20 energy groups to obtain an adequate solution to this kinetic equation.

II.3a Analytic Benchmark

An analytic benchmark for this model was desired to ensure correctness of the model. To this end, we used the results of Anderson et al [10], who showed that when D_α is chosen to be independent of r and v and that when the radial dependence of τ_{SD} is neglected, the time independent solution to Eq. (14) becomes

$$f(r,v) = \frac{\tau_{SD}}{4\pi(v^3 + v_c^3)} \sum_{n=1}^{\infty} \frac{J_0(\lambda_n r) \int_0^a S_f(r) J_0(\lambda_n r) r\, dr}{\int_0^a J_0^2(\lambda_n r) r\, dr} \left(\frac{v^3 + v_c^3}{v_0^3 + v_c^3}\right)^{\frac{\lambda_n^2 D_\alpha \tau_{SD}}{3}} \tag{16}$$

where $J_0(\lambda_n r)$ are a set of zeroth order Bessel functions labelled by $\lambda_n = \frac{c_{0n}}{a}$ with $n = 1, 2, 3; C_{0n}$ are the Bessel function zeroes and a is the plasma boundary where f vanishes. We extend Eq. (16) into a multiple energy group form by integrating it over a single energy group, i.e. $\int_{E_{j+1}}^{E_j} dE$. Also, in order to ensure a simple analytic result (for benchmarking purposes), we take the source rate to be independent of radius $S_{\alpha 0}(r) = S_{\alpha 0}$ (or equivalently, n_e and T_e have a radially uniform profile). Equation (16) becomes

$$n_{\alpha j}(r) \simeq \frac{\tau_{SD} S_f}{a} \sum_{i=1}^{\infty} \frac{J_0(r, \lambda_i)}{\lambda_i J_1(a\lambda_i)} \frac{1}{E_0^{3\gamma_i/2}} \left(E_j^{3/2} + E_c^{3/2}\right)^{\gamma_i - 1} E_j^{1/2} \Delta E \tag{17}$$

where $n_{\alpha j} \equiv \int_{v_{j+1}}^{v_j} F_\alpha d^3 v, \gamma_i = \frac{\lambda_i^2 D_\alpha \tau_{SD}}{3}$ and $\Delta E = E_i - E_{i+1}$. We set all energy group widths equal. Note that when $D_\alpha = 0$, the group density is inversely proportional to the group energy: $n_{\alpha j} \sim \frac{1}{E_j} \Delta E$. This corresponds to the classical $1/v^3$ distribution function dependence in the absence of diffusion or anomalous slowing down. On the other hand, with a large enough diffusion coefficient, the spatial loss rate can be comparable to the slowing down time. If $\frac{\lambda_1^2 D_\alpha \tau_{SD}}{3} \geq 1$, the energy group density distribution becomes inverted (see Fig. 1).

II.3b Numerical Multiple Energy Group Solution

For the ensuing numerical work we use realistic profiles of n and T. By integrating Eq. (14) over a single energy group, we obtain the discretized system of equations

$$\frac{\partial n_{\alpha j}}{\partial t} = -\frac{1}{r}\frac{\partial}{\partial r}\left[rD_{\alpha j}\frac{\partial n_{\alpha j}}{\partial r}\right] + \frac{n_{\alpha j-1}}{\tau_{s j-1}} - \frac{n_{\alpha j}}{\tau_{s j}} \qquad (18)$$

where

$$n_{\alpha j} = \int_{E_{j+1}}^{E_j} dE\, F_\alpha(v(E))$$

$$\tau_{s j} = \frac{1}{3}\tau_{SD}\ln\left[\frac{E_c^{3/2} + E_j^{3/2}}{E_c^{3/2} + E_{j+1}^{3/2}}\right].$$

In this equation, $D_{\alpha j}$ is the diffusion coefficient for fast alphas in energy group j and E_c is the critical energy [$= 32T_e$ (keV) for D-T]. The discretized energy space is constructed so that the upper boundary of group 1 corresponds to the birth energy of the alphas. Subsequent higher energy indices label correspondingly lower energy groups. Also, Eq. (18) for the highest energy group (group 1) contains the source term $S_f = 0.25n_e^2\langle\sigma v\rangle$ vice the slowing down source $\frac{n_{j-1}}{\tau_{s j-1}}$. The top of the lowest energy group, E_N, was chosen to be roughly $E_c/2$, where E_c is evaluated using the volume averaged electron temperature $\langle T_e\rangle$. The time dependent problem is solved using an implicit/explicit scheme with the initial condition that the fast alpha group densities are all zero. For each time step, the Attenberger routine solves Eq. (18) starting from the highest energy group first and then working down such that the preceding group provides a slowing down source. The spatial equation is solved by a standard finite difference routine.

Figure 1 shows two plots of group density versus energy for a fixed radius $n = a/2$. Figure 1a was generated by the discretized analytic equation (17) while the Fig. 1b plot was generated by the numerical multiple energy group scheme. With a fixed thermal background of $T_e = 10$ keV and $n_e = 2 \times 10^{20}$ m^{-3}, D_α was varied arbitrarily from 0 m^2/s to 20 m^2/sec. The plots are nearly identical, thus verifying the multi-group model. Also,

note that when $D_\alpha > 6$ m^2/s, the group density distribution becomes inverted. At these large diffusivities, alpha particles are preferentially lost prior to slowing down, thus creating a deficit of alpha particles at lower energies. Consequences of inverted alpha distributions include loss cone cyclotron instabilities, but are not further discussed here [4].

III. Calculation of η_α from the Multiple Energy Group Equations

Starting from Eqs. (3a) and (15) which yields

$$\eta_\alpha(r) = 1 + \frac{1}{E_{\alpha 0} S_f} \int_0^{v_0} d^3 v_\alpha \frac{m_\alpha v_\alpha^2}{2} \frac{1}{r} \frac{\partial}{\partial r} \left(r D_\alpha(r,v) \frac{\partial f_\alpha}{\partial r} \right) \tag{19}$$

we discretize this into the following form

$$\eta_\alpha(r) = 1 + \frac{1}{E_{\alpha 0} S_F} \sum_{j=1}^{N} E_j \frac{1}{r} \frac{\partial}{\partial r} \left(r D_{\alpha j}(r) \frac{\partial n_j(r)}{\partial r} \right). \tag{20}$$

This provides an expression for the radially dependent α power coupling efficiency and is constructed with the output from the multiple energy group code. We recognize that it is possible for $\eta_\alpha(r)$ to be greater than one in the outer part of the plasma since the inner part of the plasma, which has a large source of fusion alphas, provides to the outer plasma a source of alphas as they diffuse outward. This flux of alphas from the core continues to thermalize in the outer region, giving up energy to the plasma despite the low fusion rate.

Of more practical interest is the volume averaged η_α defined as

$$\langle \eta_\alpha \rangle \equiv \frac{\langle \eta_\alpha(r) P_{\alpha 0}(r) \rangle}{\langle P_{\alpha 0}(r) \rangle} \tag{21}$$

where $\langle x \rangle$ represents the volume average of x and $P_{\alpha 0}(r) \equiv E_{\alpha 0} S_f$. Equation 21 then becomes

$$\langle \eta_\alpha \rangle = 1 + \frac{a \sum_j E_{\alpha j} D_{\alpha j} \frac{\partial n_j}{\partial r} \Big|_{r=1}}{E_{\alpha 0} \int_0^a dr \, r S_{\alpha 0}(r)}. \tag{22}$$

10

It should be emphasized that in this expression $\frac{\partial n_j}{\partial r}\big|_{r=a}$ is not a prescribed boundary condition. Rather, it reveals that the volume averaged η_α is determined by the gradient of the alpha density at the boundary which is in itself determined by the solution of the differential equation, Eq. (18). At steady state, $\langle\eta_\alpha\rangle$ rises from 0 (total diffusive α loss) to 1 (no diffusive loss).

IV. Results

The choice of D_α can either be taken from experiments or determined from theory. Experimental results for $D_\alpha(r, E)$ are far from being complete, and those for a burning or ignited plasma are presently nonexistent.

IV.1 Constant D_α

The multiple energy group code is run for several different values of constant D_α. Figure 2 shows that significant degradation of η_α occurs for values of D_α greater than or equal to 1 m^2/s. This is not surprising since, for $D_\alpha > 1$ m^2/s, $1/\nu_L$ becomes on the order of or smaller than τ_{SD}. The profile of the radial η_α is shown in Fig. 3 which reveals its increasing nature near the boundary.

IV.2 Theoretical D_α

In recent years, alpha particle interaction with Alfvén modes has come under intense study. In Ref. [14], a stochastic α diffusion coefficient due to the kinetic Alfvén wave was given. Recently, F. Gang [15] and H. Biglari [16] have calculated diffusion related coefficients of the form [15]

$$D_\alpha \propto \beta_\alpha \frac{\omega \alpha^*}{\omega_A}\left[1 - \frac{\omega}{\omega_\alpha^*}\right]^2 \tag{23}$$

11

where $\omega_A = k_\parallel v_\alpha \sim \frac{v_A}{R}$ is the Alfvén frequency

$$\omega_\alpha^* = k_\theta \frac{T_\alpha \left| \frac{\partial N_\alpha}{\partial r} \right|}{e_\alpha N_\alpha B}$$

is the α diamagnetic frequency. Thus, D_α^{an} is strongly nonlinearly dependent on $\partial n_\alpha / \partial r$ itself! For more detail on D_α see Appendix A. These theories treat only the velocity averaged total density

$$N_\alpha = \sum_{j=1}^{N_j} n_{\alpha j}.$$

We inserted this form of anomalous diffusion D_α^{an} into the multiple energy group equation for $n_{\alpha j}$. With a fixed set of thermal background parameters corresponding to the "technology phase" ITER, a constant minimum $D_{\alpha 0} = 0.2$ m^2/sec was added to prevent $D_\alpha \to 0$, so that the total diffusion coefficient was $D_\alpha = D_{\alpha 0} + D_\alpha^{an}$. A comparison is made with the case where only a constant $D_\alpha = D_{\alpha 0}$ is applied. For both cases, a steady state $n_\alpha(r)$ distribution is reacted after ~ 2 sec as shown in Fig. 4. As can be seen in Fig. 5, the diffusion at the center equals the background level of 0.2 m^2/s, increasing to a peak of $D_\alpha \approx 1$ m^2/s at a radius of $r = a/2$ (where the slope of alpha density is greatest) and then dropping in the outer region. The difference in the resulting volume averaged coupling efficiency defined in (22) $\langle \eta_\alpha \rangle$ is less dramatic; taking only a constant (neoclassical level) $D_{\alpha 0}, \langle \eta_\alpha \rangle = 0.99$. Taking the full $D_{\alpha 0} + D_\alpha^{an}, \langle \eta_\alpha \rangle = 0.94$. Including the time dependence in the multi-group diffusion equation with the theoretical D_α^{an} of Eq. (23) results in Fig. 6. The oscillation of D_α settling to a steady state value after $t = 1$ sec is a consequence of the nonlinear dependence of D_α on $\partial n_\alpha / \partial r$. A steady state value for D_α and its self-consistent $\partial n_\alpha / \partial r$ occurs at such a value that the fusion source term S_f (which tends to centrally peak $n_\alpha(r)$) is balanced by the outward diffusion due to D_α. Since the problem is cubic in $\partial n_\alpha / \partial r$, other possibly oscillatory solutions exists. This matter is presently under investigation.

12

Figure 7 shows the parametric dependence of the volume averaged α coupling efficiency with electron temperature. As discussed before, the scaling of η_α shown in Eqs. (4a,b) explains most of the sharp drop-off with increasing T_e, but the T_e dependence of D_α^{an} is also included here. This result would favor a high density, low T_e mode of operation.

IV.3 Effects on Plasma Operations Contours

To examine the effects of our calculated η_α on the thermal equilibrium of a high Q machine like ITER, we start with the steady state 0-D power balance

$$\frac{\partial}{\partial t}\left[\frac{3}{2}\sum_{k=i,e,z} n_k T_k\right] = 0 = \eta_\alpha P_{\alpha 0} + P_\Omega + P_{aux} - P_{loss} - P_{rad} \tag{24}$$

where all quantities are volume averaged and are in general a function of T_e and n_e, including η_α. The effect of η_α is a decrease in the input contribution from the alpha power. A useful approach is to plot contours of physically relevant quantities on a plot of n_e versus $T_e = T_i = T$. Contours of P_{aux}, thermonuclear Q, β_{crit}, and $\langle\eta_\alpha\rangle$ can be produced by solving Eq. (14), given the temperature and density. Fig. 8a shows the standard operations contours for perfect α heating efficiency $\eta_\alpha = 1$ (we used the "physics phase" parameters of ITER, i.e. $D_\alpha = 0$).

An examination of the $\eta_\alpha < 1$ contours in Fig. 8b reveals that, given a constant D_α, η_α decreases with electron temperature, but increases with electron density, consistent with Eq.(12). For $D_\alpha = 3$ m^2/s, η_α can be affected ($\simeq 0.9$) for typical densities. The ITER ignition regime exists near $\langle T_e\rangle = 10$ keV.

When $\eta_\alpha < 1$, the thermonuclear amplification $Q \equiv P_{fusion}(out)/P_{aux}(in)$ is reduced at constant $n\tau_E T$, i.e. machine design and bulk plasma performance. This was shown in Ref. [5], Fig. 3, which is shown here for convenience as our Fig. 9. (Reference [24] as quoted in this figure is to D. R. Cohn, MIT Report PFC/JA-90-6.)

V. Summary and Conclusion

After qualitatively introducing the relationship between a nonzero anomalous diffusion coefficient D_α^{an} and the α heating efficiency η_α, a reduced drift kinetic equation for the α distribution function $F_\alpha(r, E, t)$ was derived containing partial derivatives with respect to all of these variables. This equation is solved by a multi-energy group method for $\{E_j\}$, each of which is (nonlinear) diffusion equation in r and t.

The method is first validated with a constant, prescribed diffusion coefficient. Then, a theory based D_α^{an} is introduced from a self-consistent α particle Alfvén wave turbulence solution given in Eq. (23), whose diffusion coefficient depends itself on $\partial n_\alpha / \partial r$. The consequences of this model for the spatial temporal dependence of D_α and η_α are developed, including the effect on the plasma operations contours of an ITER-like fusion reactor. One finds that for $D_\alpha^{an} \sim 1$ m²/s, the α coupling efficiency is reduced to $\eta_\alpha \sim 0.9$. This affects the thermonuclear amplification factor Q. Relatively low T_e, high n_e operation mitigates this coupling loss. The nonlinear relaxation of the coupled $D_\alpha^{an}, \partial n_\alpha / \partial r$ can lead to oscillations in both quantities, on a mix of time scales determined by $\tau_{SD}, (4D_\alpha^{an}/a^2)^{-1}$ and S_f, the fusion source strength. While the theoretical models for D_α^{an} will improve over time and become validated on TFTR and JET, the possible design impact of a $D_\alpha^{an} > 1$ m²/sec for an ITER-like machine should be allowed for.

Acknowledgments

References

[1a] A. Mikhailovskii, T. Kaladze, private communication 1975.

[1b] M. N. Rosenbluth, P. H. Rutherford, Phys. Rev. Lett. **34** (1975) 1428.

[2] D. J. Sigmar, H. C. Chan, Nucl. Fus. **18** (1978) 1569.

[3] K. T. Tsang, D. J. Sigmar, J. Whitson, Phys. Fluids **24** (1981) 1508.

[4] W. Sutton, D. J. Sigmar, G. Miley, Fusion Techn. **7** (1985) 374.

[5] D. J. Sigmar and CIT Team, Plas. Phys. Contr. Nucl. Fus. Res. 1990, p. 455, Vol. III, Vienna 1991.

[6] D. J. Sigmar, H. C. Chan, Nucl. Fus. **18** (1978) 1569.

[7] D. Düchs, D. Pfirsch, Plas. Phys. Contr. Nucl. Fus. Res., 1974, Vol. I. , p. 669 (5th IAEA Conf. , Tokyo).

[8] G. Kamelander, Fusion Techn. **18** (1990) 384, also paper presented at the IAEA alpha particle conference, Aspenas 1991 (to appear in Physica Scripta).

[9] E. Attenberger, W. Houlberg, Nucl. Techn. Fusion **4** (1984) 183.

[10] D. Anderson, P. Batistoni, M. Lisak, Nucl. Fus. **31** (1991) 2147.

[11] A. A. Ware, Phys. Fluids **27** (1984) 1215.

[12] C. T. Hsu, P. J. Catto, D. J. Sigmar, Phys. Fluids **B2** (1990) 280.

[13] V. Ya. Goloborodko, V. A. Yavorskii, Fusion Techn. **18** (1990) 414.

[14] K. Tsang, D. J. Sigmar, J. Whitson, Phys. Fluids **24** (1981) 1508.

[15] F. Gang, "Alpha Particle Driven Alfvén Wave Turbulence," accepted for publication in Phys. Fluids **B4** (1992).

[16] H. Biglari, "Collective α Particle Losses due to Alfvén Wave Turbulence," private communication, 1991.

Appendix A

In Ref. [15], F. Gang develops the α particle diffusion due to Alfvén turbulence with the saturation amplitude governed by ion Compton scattering in the bulk plasma. In Eq. (51) he finds

$$D_\alpha^{an} = 0.1 c_s \rho_s \frac{n_\alpha}{n_e} \left(\frac{T_\alpha}{T_e}\right)^2 \left(\frac{\rho_s}{R}\right)^2 \left(\frac{\Omega_i}{\omega_A}\right) \left(\frac{L_n^i}{L_n^\alpha}\right) \left(\frac{\overline{k}_\perp \rho_\alpha}{k_\parallel R}\right)^2 \left(1 - \frac{\omega_A}{\omega_{*\alpha}}\right)^2$$

$$\frac{\overline{k}_\theta}{\langle k_\theta \rangle - \overline{k}_\theta} \frac{\overline{k}_\theta^2}{\langle k_r \rangle^2}.$$

Here, c_s is the sound speed, ρ the gyroradius, Ω_i the ion gyroradius, $L_n^j = \left(\frac{1}{n_j} \frac{dn_j}{dr}\right)^{-1}$, R the major radius, ω_A the Alfvén frequency, and the last two factors are certain spectrum averaged wave vectors of the kinetic Alfvén wave turbulence defined in [15]. Evaluating these expressions for ITER-like parameters yields $D_\alpha \simeq 1 \ \mathrm{m^2/s}$.

Figure Captions

1a α energy group density versus energy for $D_\alpha = 0, 3, 6, 15$ and 20 m^2/s. Analytic solution. Note slope inversion for $D_\alpha > 6$ m^2/s.

1b Same as Fig. 1a multi-energy group numerical solution. The agreement is good.

2 Volume averaged α coupling efficiency $\langle \eta_\alpha \rangle$ versus D_α.

3 Local $\eta_\alpha(r)$ versus plasma radius. Locally, v$\eta_\alpha > 1$ is possible since $\eta_\alpha(r) = P_\alpha(r)$ coupled into the bulk plasma$/P_{\alpha 0}(r)$, the α birth power.

4 Alpha density versus time, for the theoretical model D_α^{an} for various plasma radii.

5 D_α^{an} versus radius. The maximum occurs at the coupled maximum of $\partial n_\alpha / \partial r$.

6 Temporal behavior of D_α^{an}. The first rise is due to fusion reaction driven peaking of $n_\alpha(r, t)$. When $\partial n_\alpha / \partial r$ is large enough strong diffusion flattens the slope until a balance is reached.

7 $\langle \eta_\alpha \rangle$ as a function of T_e and n_e, for the theoretical model D_α^{an}. Part of the shown trends originate from the classical scaling of $\tau_{SD} \sim T_e^{3/2}/n_e$, part of it from the scalings of D_α^{an}. High n_e, low T_e provides a larger α coupling efficiency.

8a Standard plasma operations contour plot for ITER, assuming perfect α coupling efficiency, $\langle \eta_\alpha \rangle = 1$.

8b Same plot, for $D_\alpha^{an} = 3$ m^2/sec. The additional curves depict constant $\langle \eta_\alpha \rangle < 1$ contours. As noted in Fig. 7, high n_e, low T_e increases $\langle \eta_\alpha \rangle$.

9 Thermonuclear Q versus ignition margin, for different values of $\langle \eta_\alpha \rangle$. For a given ignition margin $\lesssim 1$, a drop in $\langle \eta_\alpha \rangle$ produces a large drop in Q. (From Ref. 9.)
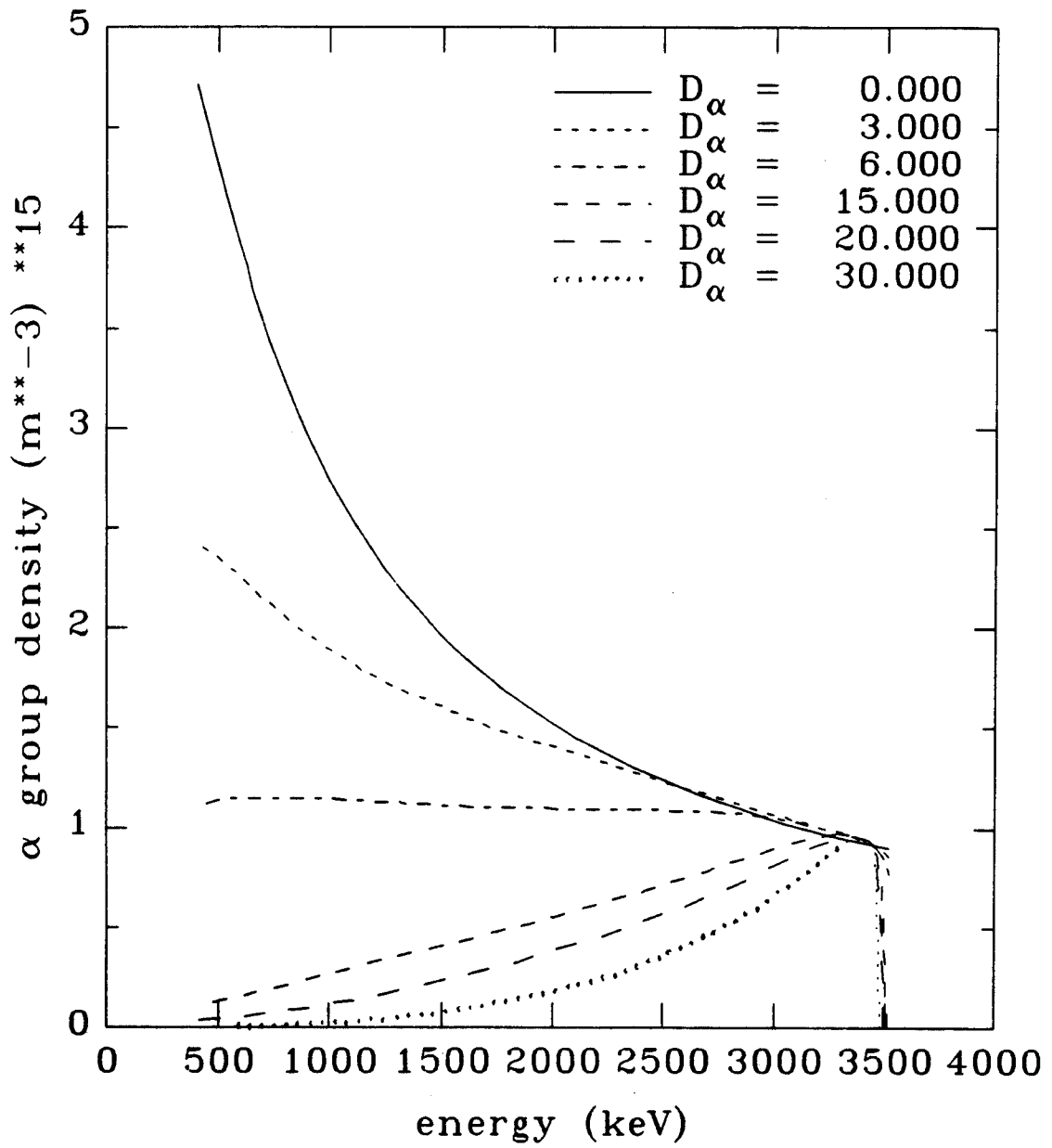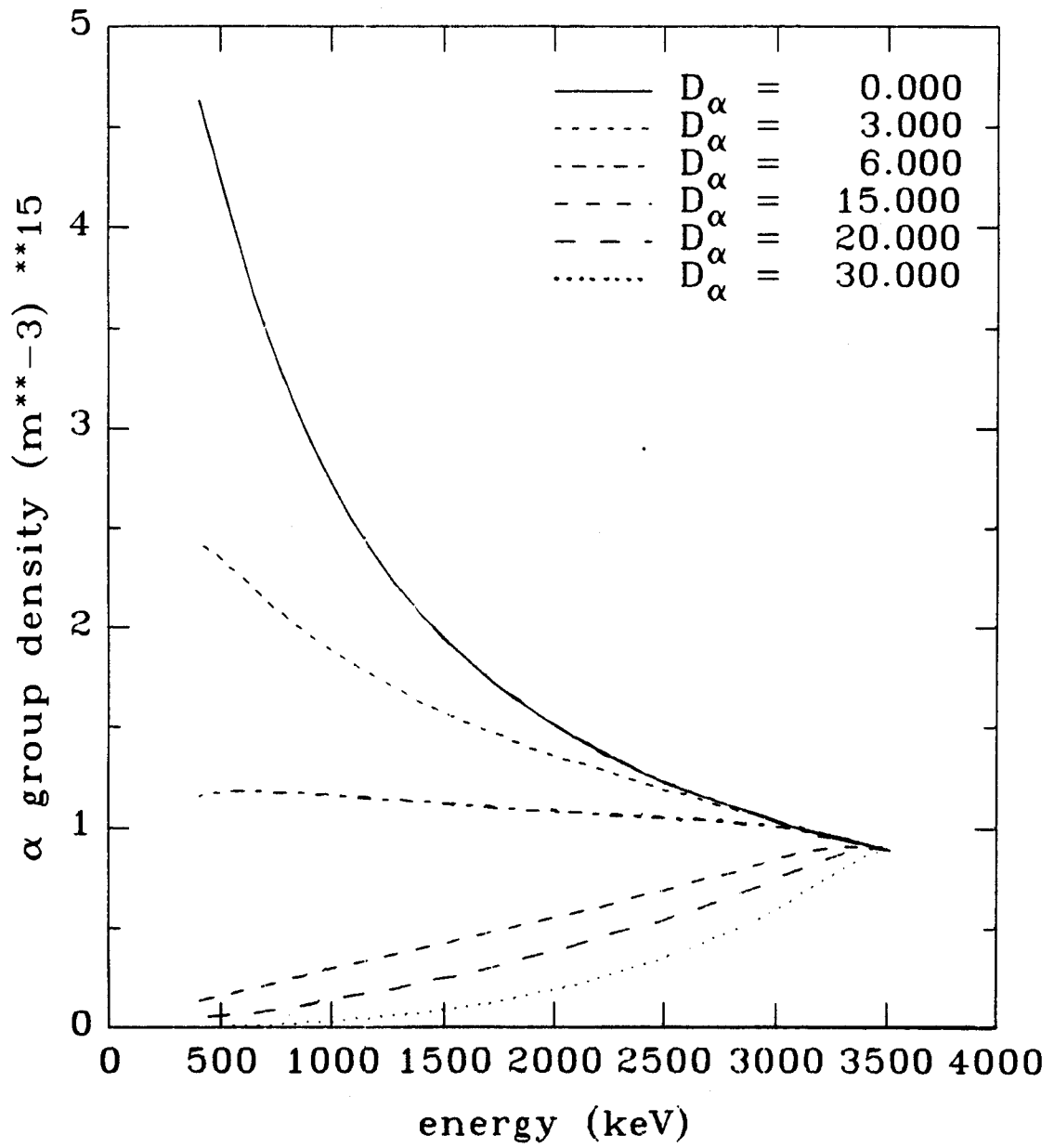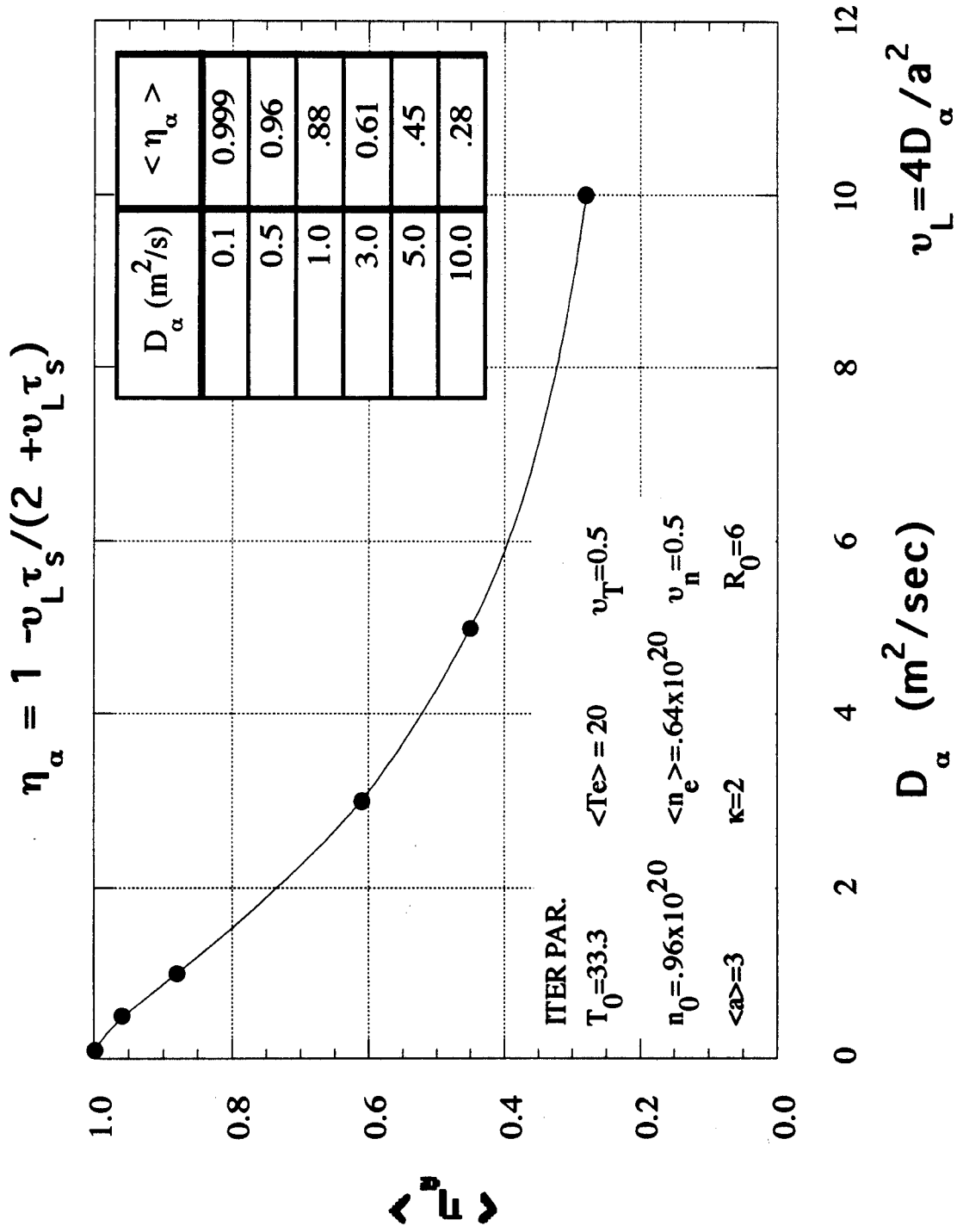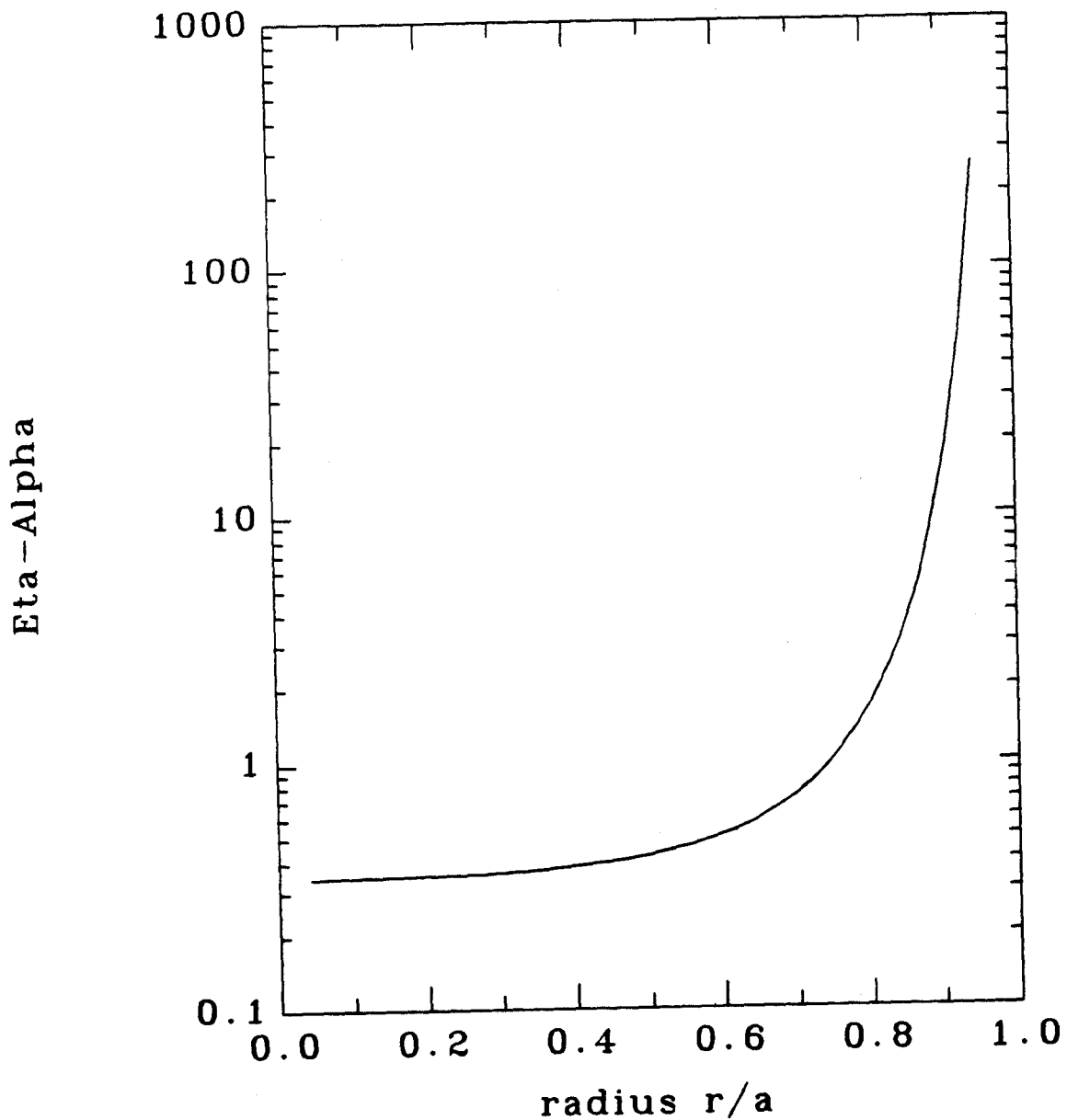
Figure 1a

Figure 1b

$$\eta_\alpha = 1 - v_L \tau_s / (2 + v_L \tau_s)$$

D_α (m^2/s)	$\langle \eta_\alpha \rangle$
0.1	0.999
0.5	0.96
1.0	.88
3.0	0.61
5.0	.45
10.0	.28

ITER PAR.

$T_0 = 33.3$ $\langle Te \rangle = 20$ $v_T = 0.5$

$n_0 = .96 \times 10^{20}$ $\langle n_e \rangle = .64 \times 10^{20}$ $v_n = 0.5$

$\langle a \rangle = 3$ $\kappa = 2$ $R_0 = 6$

$v_L = 4 D_\alpha / a^2$

D_α (m^2/sec)

$\langle \eta_\alpha \rangle$

Figure 2

ITER - technology phase
$\langle T_e \rangle = 20 \, keV, \langle n_e \rangle = .64 \times 10^{20}$

$D_\alpha = 3 \, m^2/s = const$

$\langle T_e \rangle = 20 \, keV$ $\nu_T = 1$ 400 time steps
$\langle n_e \rangle = .64 \times 10^{20} \, m^{-3}$ $\nu_n = 2$ $T_{end} = 2 \, s$
$a = 2.15 \, m$ $\kappa = 2$ 50 spatial nodes
$\langle a \rangle = 3 \, m$ 20 energy groups
$R_0 = 6 \, m$ $E_{nj} = 200 \, keV$ Figure 3
$B_0 = 4.8 \, T$ $\Delta E = 175 \, keV$
$Z_{eff} = 2.2$ $D_\alpha = D_{\alpha_0} = 3 \frac{m^2}{s}$
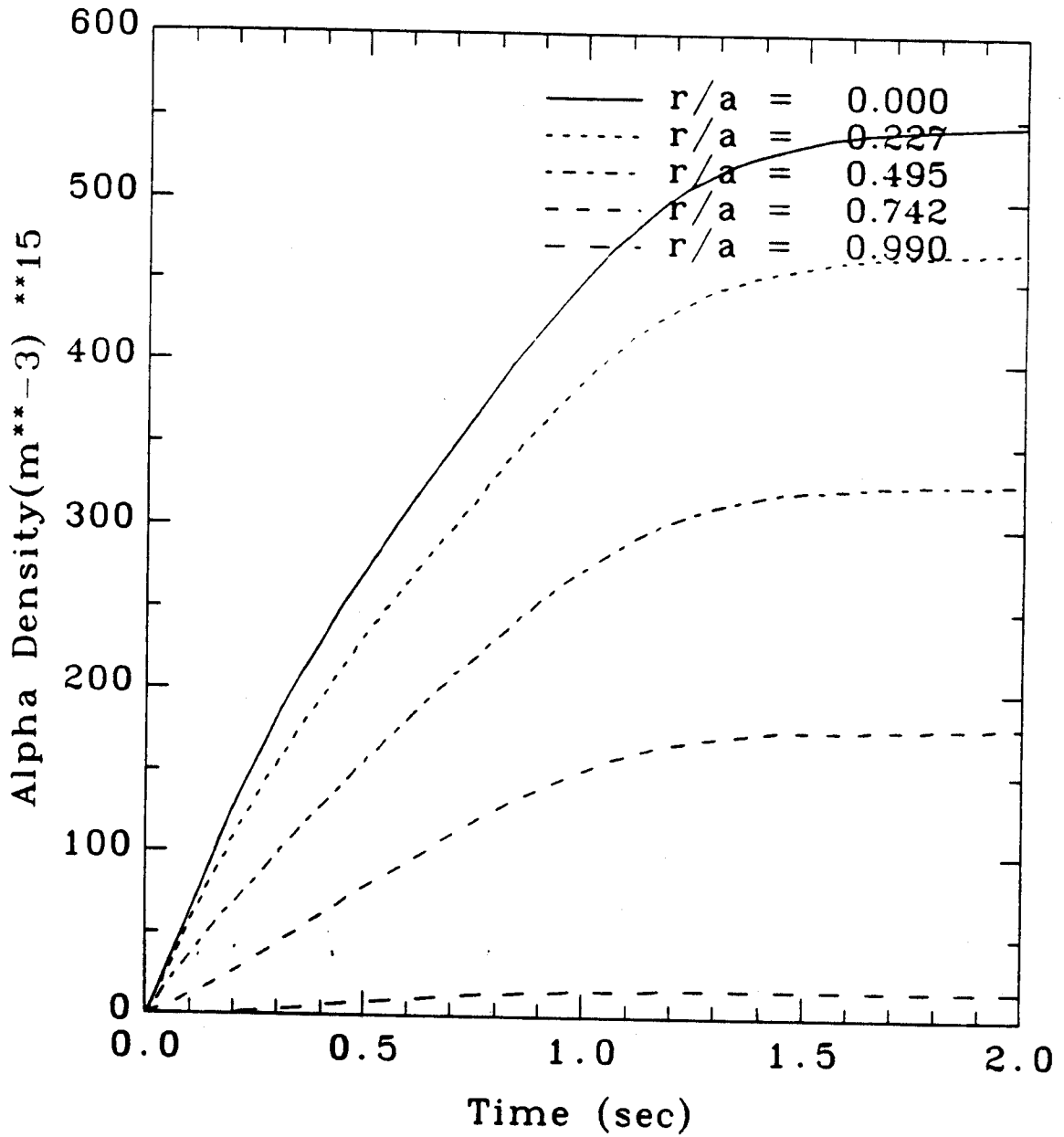
$$D_\alpha = .2 \, m^2/s + D_\alpha^{anom}$$

Figure 4

$$\langle \eta_\alpha \rangle = .97$$

$$D_{\alpha 0} = .2 \; m^2/s$$

$$D_\alpha = D_{\alpha 0} + D_\alpha^o$$

$$D_\alpha^{an} \propto (k_\theta^2 \rho_\alpha^2) \frac{\beta_\alpha}{L_{p\alpha}} \left(\frac{\omega_{*\alpha}}{\omega_A} - 1 \right)^2$$
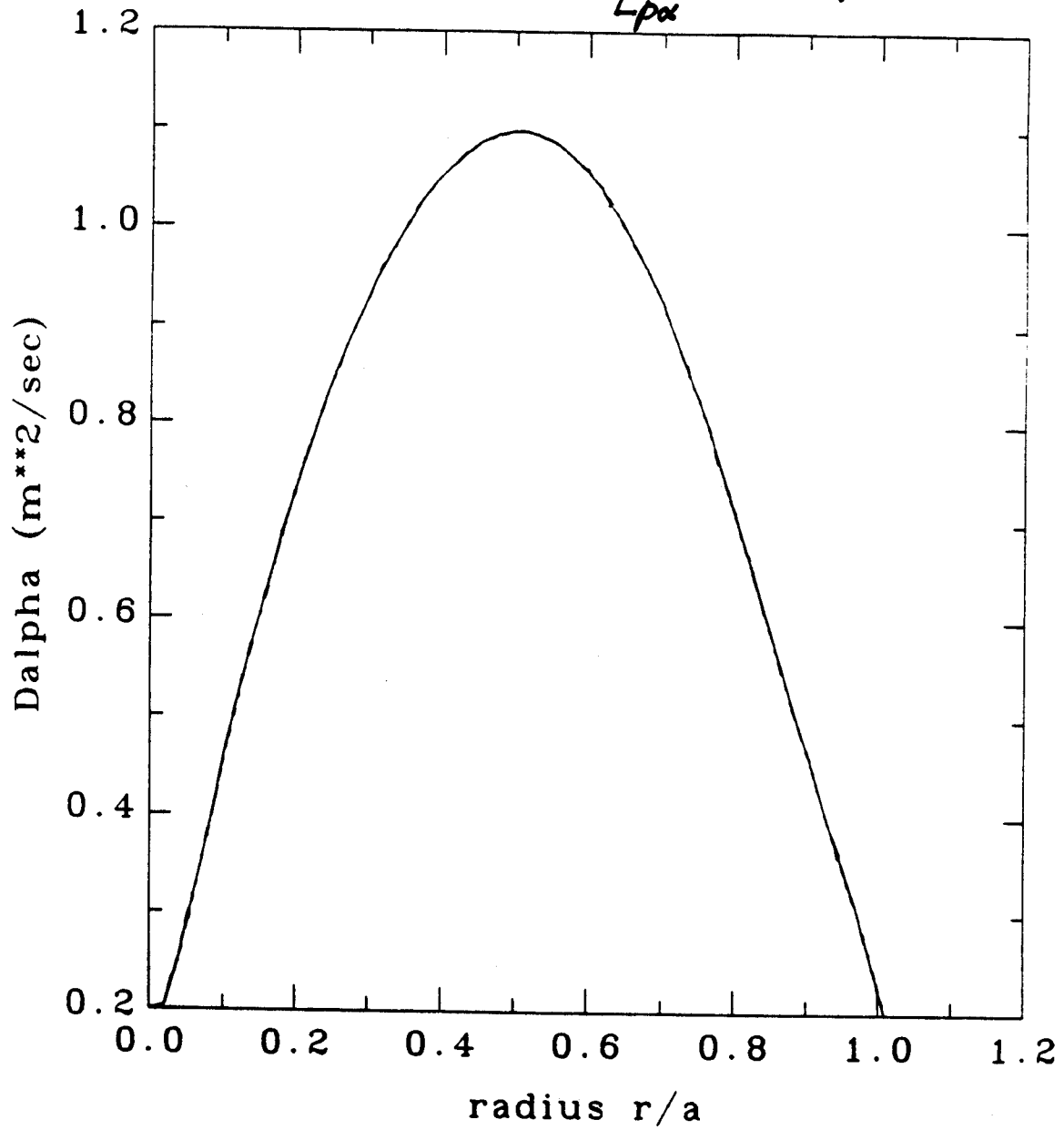
Figure 5

$$D_\alpha = .2 \ m^2/s + D_\alpha^{anom}$$

Figure 6

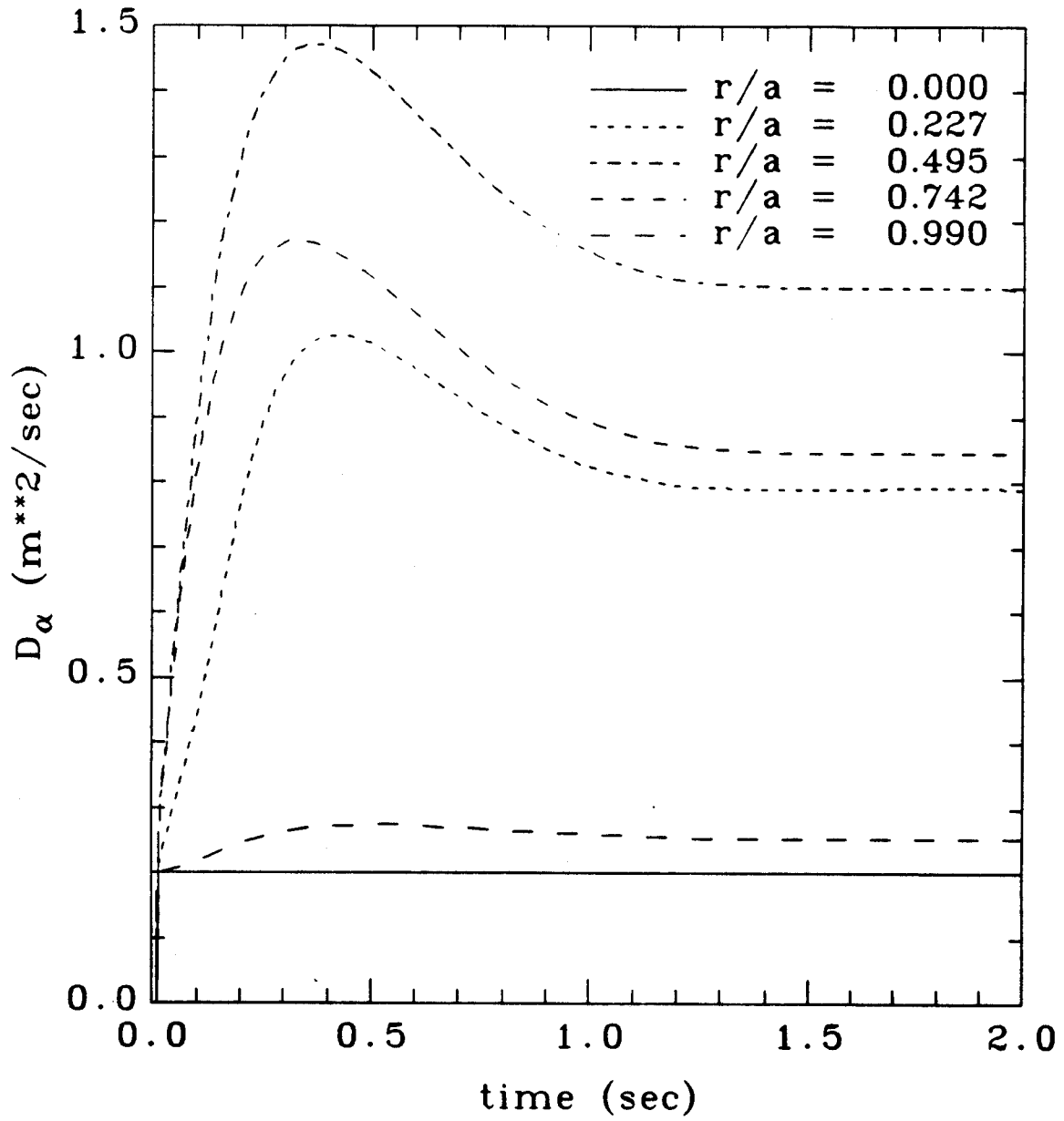$$D_\alpha = .2 \ m^2/s \ + \ D_\alpha^{an}$$

Legend:
	⟨ele dens⟩ =	×10²⁰	
——	⟨ele dens⟩ =	0.200	m**−3
······	⟨ele dens⟩ =	0.525	m**−3
—·—	⟨ele dens⟩ =	0.850	m**−3
— —	⟨ele dens⟩ =	1.175	m**−3
— — ·	⟨ele dens⟩ =	1.500	m**−3

Vertical axis: ⟨eta−alpha⟩

Horizontal axis: ⟨electron temperature⟩ Te (keV)

Right-side annotations:
$D_\alpha = .2 \frac{m^2}{s} + C$
$f_{He} = .083$
$f_z = .0345$
$z = 6$
$Z_{eff} = 2.2$
$a = 2.15.$
$R_o = 6m$
$\kappa = 2$
$B = 4.8T$
$I = 19 \ MA$
$SCALE \ ITE.$
$Hmode = 2.$
$a_n = .5$
$D_T = 1$

Figure 7

Figure 8a

(Physics Phase) CDA

Curves of const. η_α and
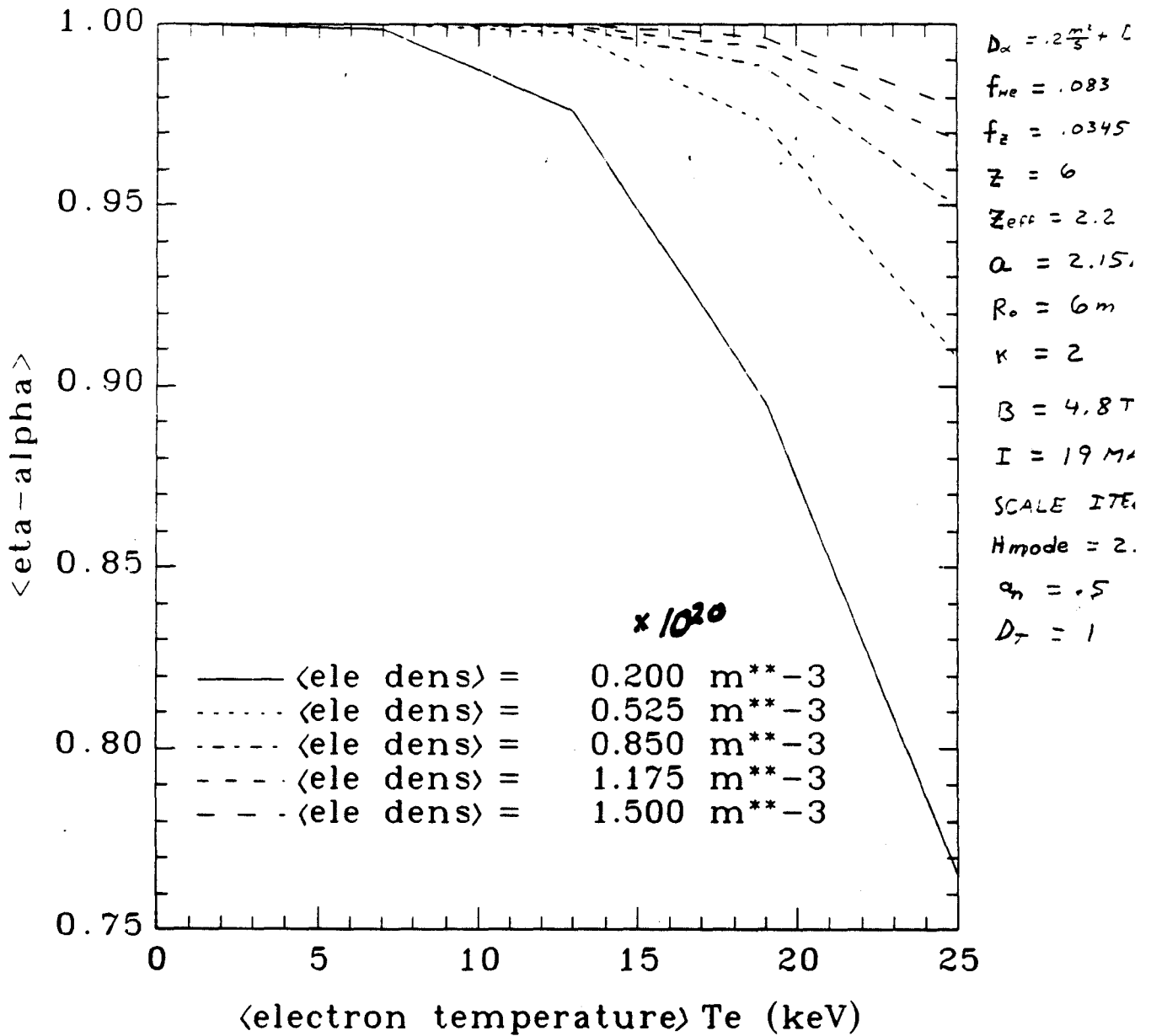
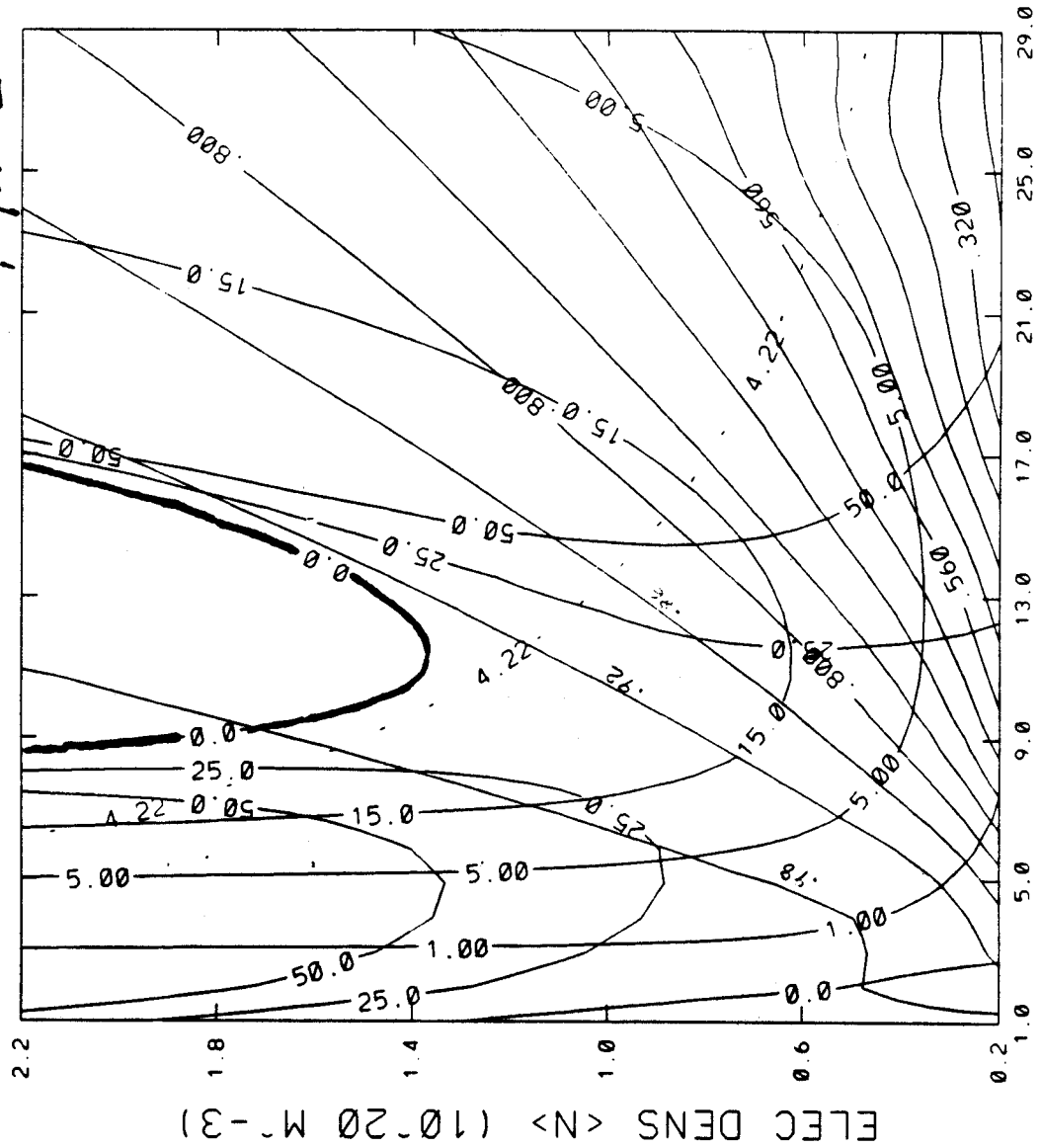St. State τ_{aux}- and Q-contours, $\eta_\alpha < 1$

AUX PWR CONTOURS (MW) - SOLID

TROTON BETA LIMIT - DOTTED

POPALF OUTPUT

Dalph = 3.00 m^-2/sec

FASH = 0.083

FZ = 0.0178

Z = 6.00

a = 2.15 m

kapa = 2.00

R = 6.00 m

B = 4.85 tesla

I = 22.00 MA

SCAL = ITER89P

HMODE = 2.00

NEWN = 0.50

NEWT = 1.00

ELEC TEMP <nT>/<n> (KEV)

ELEC DENS <N> (10^20 M^-3)

Figure 8b

Figure 9